Influence of heterogeneities of density on the hydromechanical behaviour of pellet-based bentonite materials in imbibition experiments

Benjamin Darde, Anh Minh A.M. Tang, Jean-Michel Pereira, Patrick Dangla, Jean-Noël Roux, Baptiste Chabot, Jean Talandier, Minh Ngoc Vu

▶ **To cite this version:**

Benjamin Darde, Anh Minh A.M. Tang, Jean-Michel Pereira, Patrick Dangla, Jean-Noël Roux, et al.. Influence of heterogeneities of density on the hydromechanical behaviour of pellet-based bentonite materials in imbibition experiments. Applied Clay Science, 2022, 216, pp.106353. 10.1016/j.clay.2021.106353 . hal-03905469

HAL Id: hal-03905469

https://enpc.hal.science/hal-03905469

Submitted on 18 Dec 2022

HAL is a multi-disciplinary open access archive for the deposit and dissemination of scientific research documents, whether they are published or not. The documents may come from teaching and research institutions in France or abroad, or from public or private research centers.

L'archive ouverte pluridisciplinaire **HAL**, est destinée au dépôt et à la diffusion de documents scientifiques de niveau recherche, publiés ou non, émanant des établissements d'enseignement et de recherche français ou étrangers, des laboratoires publics ou privés.

Copyright

Title:

Influence of heterogeneities of density on the hydromechanical behaviour of pellet-based bentonite materials in imbibition experiments

Authors:

Benjamin Darde[1,2]: benjamin.darde@enpc.fr

Anh Minh Tang[1]: anh-minh.tang@enpc.fr

Jean-Michel Pereira[1]: jean-michel.pereira@enpc.fr

Patrick Dangla[1]: patrick.dangla@univ-eiffel.fr

Jean-Noël Roux[1]: jean-noel.roux@univ-eiffel.fr

Baptiste Chabot[1]: baptiste.chabot@enpc.fr

Jean Talandier[2]: jean.talandier@andra.fr

Minh Ngoc Vu[2]: minh-ngoc.vu@andra.fr

Affiliations:

[1]: Navier, Ecole des Ponts, Univ Gustave Eiffel, CNRS, Marne-la-Vallée, France

[2]: French national radioactive waste management agency (Andra), France

Corresponding author:

Anh Minh Tang

Ecole des Ponts ParisTech

6-8 avenue Blaise Pascal

Cité Descartes – Champs-sur-Marne

77455 Marne-la-Vallée cedex 2

anh-minh.tang@enpc.fr

Abstract:

An experimental investigation on the hydromechanical behaviour of pellet-powder mixtures, candidate materials for sealing the galleries in radioactive waste disposal concepts, was described. Imbibition experiments were performed using a specially-designed column, with square cross-section and glass sides allowing pictures to be taken by a camera. Relative humidity and swelling pressure were measured at different elevations of the column. Three mixtures with an identical pellet volume fraction and various powder volume fractions were used to study the influence of heterogeneities of density on the hydromechanical behaviour of the mixture under repository conditions. Results demonstrated that hydration of the material was dominated by water vapour flux, with pellets and inter-pellet pores not at hydraulic equilibrium. In mixtures with low powder content, the evolution of swelling pressure was controlled by contact forces between pellets. The material progressively lost the initial granular structure upon hydration. Note that hydration was made by imbibition, instead of injecting liquid water at high pressure, to avoid unrealistic liquid water flow rates in the initial large inter-pellet voids. In addition, sensors four times larger than the pellets were used to measure a representative value of swelling pressure.

Keywords:

Bentonite, Pellet mixture, Imbibition experiment, Swelling pressure, Relative humidity, Water migration

Funding:

This work was funded by École des Ponts ParisTech and the French National Agency for Radioactive Waste Management (Andra).

1. Introduction

Bentonite materials have been considered as sealing materials in radioactive waste disposal concepts of the French National Agency for Radioactive Waste Management (Andra) for their low permeability, good radionuclide retention capacity and ability to swell upon hydration (Andra, 2005). In the gallery, the bentonite swelling in the radial direction is prevented by the host rock and a swelling pressure develops. This latter contributes to the sealing of fractures in the excavation damaged zone. Experimental studies demonstrated that the permeability and swelling pressure of a bentonite material in fully-saturated state were related to its dry density (Karnland et al., 2006; Lloret and Villar, 2007; Wang et al., 2012; Kaufhold et al., 2015).

Owing to operational convenience, pellet-based bentonite materials have been regarded as candidate materials for the swelling clay plug and backfill (Imbert and Villar, 2006; Dixon et al., 2011; Bosgiraud and Foin, 2016; Sánchez et al., 2016; Darde et al., 2018; Bernachy-Barbe et al., 2020; Sellin et al., 2020). In these studies, the galleries were expected to be filled with pellet-based mixture. Screw auger can be used for this purpose as demonstrated by Andra in a full-scale experiment (Noiret et al., 2016). During the installation of the granular mixture in the gallery, heterogeneities of dry density can develop. Obtaining a homogeneous mixture was found difficult in a full-scale experiment (Noiret et al., 2016) as well as in the laboratory Molinero Guerra et al. (2017).

Following its installation, the material will be progressively hydrated by the pore water of the host rock. Upon hydration, experimental studies at the laboratory scale (Hoffmann et al., 2007; Darde et al., 2020a) and discrete element method (DEM) simulations (Darde et al., 2021, 2020b) suggested that the evolution of swelling pressure depended on the arrangement of the particles (pellets and powder grains). This initial granular structure became less obvious during hydration (van Geet et al., 2005; Hoffmann et al., 2007; Molinero Guerra et al., 2018a; Darde et al., 2020a; Villar et al., 2021).

In order to demonstrate the influence of the initial granular structure and progressive homogenisation of the mixture on the performance of the seals in the repository, the present work aims at investigating the hydromechanical behaviour of bentonite pellet mixtures in the course of hydration using imbibition columns. A total of three imbibition experiments were performed on three different pellet and powder mixtures, one of them is a candidate sealing material in the French concept for radioactive waste disposal (Noiret et al., 2016), using hydration columns.

Several imbibition experiments performed on pellet materials have been described in the literature (Imbert and Villar, 2006; Molinero Guerra et al., 2018a, 2018b; Bernachy-Barbe et al., 2020). The originality of the tests described in the present work stems from the following points: (*i*) columns with a square cross-section and glass sides were especially designed for the study, allowing a direct observation of the soil texture changes during hydration; (*ii*) hydration was performed through imbibition of water instead of injection of water, to avoid significant water flow rates in the inter-pellet space, reproducing repository conditions more realistically and avoiding an early loss of the granular structure (actually, in the case of Andra's concept, water flows from the host rock, claystone with very low permeability, with negligible pressure during the re-saturation phase); (*iii*) swelling pressure was measured using sensors of diameter four times as large as the pellet diameter, providing rather an average value than local ones as with pellet-sized sensors (Darde et al., 2021). This issue actually is a critical point, since the duration of hydration tests performed on bentonite materials is significant, and the opportunity to perform several tests is thus very limited, so high variability of the measurement can affect the interpretation of results.

2. Materials and Method

2.1. Pellets and powder

The materials in this study were provided by Laviosa MPC, France. Pellets were made of MX80 sodium bentonite. Its mineral composition is given in Table 1. Its cation exchange capacity (CEC), specific surface area (S_{SA}), and amount of Na^+ and Ca^{2+} cations in interlayer space are presented in Table 2. Pellets had a subspherical shape, with a cylinder-shaped part and two spherical caps at the top and

bottom (Figure 1). The pellet's properties are presented in Table 3; additional data can be found in Molinero Guerra et al. (2017) and Darde et al. (2018).

Table 1. Mineral composition of the MX80 bentonite from X-ray Diffractometer. Data from Laviosa MPC, cited by Molinero-Guerra et al. (2017).

Mineral	Mass proportion
Pyrite	< 1%
Montmorillonite	80%
Albite	2%
Anorthite	8%
Quartz	4%
Muscovite	4%

Table 2. Properties of the MX80 bentonite. Data from Saiyouri et al. (2004)

CEC	82.3	meq/100 g
S_{SA}	522	m^2/g
Na^+	80	meq/100 g
Ca^{2+}	5	meq/100 g

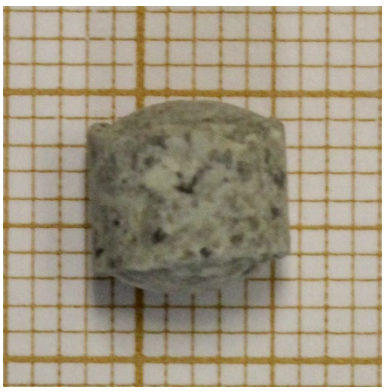

Figure 1. Picture of a pellet. The size of each square on the picture is 1 mm × 1 mm.

Table 3. Properties of pellet.

Pellet properties	**Value**
Geometrical properties	
Diameter[a]	7 mm
Height of the cylinder part[a]	5 mm

Total height[a]	7 mm
Curvature radius of the spherical caps[a]	6.5 mm
Physical properties	
Density of solid particles[b]	2.77 Mg/m^3
Initial dry density[a]	1.91 Mg/m^3
Initial void ratio[a]	0.45
Initial suction[a]	89 MPa
Initial water content[a]	12%

a: Darde et al. (2018); b: Saba et al. (2014)

The powder was obtained by crushing pellets ("Concassé d'expangel SP32" following the nomination of the producer, Laviosa MPC). The initial suction and water content of the powder were 180 MPa and 3.5%, respectively. The average diameter of the powder grains was 0.65 mm (Molinero Guerra et al., 2017) which was ~10 times smaller than the pellets.

2.2. Pellets-powder mixtures

Three mixtures of pellets and powder were used in the imbibition experiments. The reference mixture was a pellet-powder mixture in proportion 70/30, respectively, in dry mass, a candidate sealing material in the French concept of radioactive waste disposal. The dry density of the mixture, ρ_d, was 1.50 Mg/m^3. The pellet initial volume fraction (volume of pellets / total volume), ϕ_{p0}, was 0.553. The powder initial volume fraction (volume of powder grains / total volume), ϕ_{g0}, was 0.236. During the installation of the mixture in the galleries, powder might trickle through the inter-pellet space, causing local heterogeneities. To investigate the influence of heterogeneities of density resulting from powder trickling on the mixture behaviour, two other mixtures were studied. These mixtures had a value of ϕ_{p0} identical to that of the 70/30 reference mixture, but different values of ϕ_{g0}. These mixtures are referred to as "70/15" and "70/0" to indicate the identical pellet volume fraction and reduced powder volume fraction. The properties of the mixtures are summarised in Table 4.

The material is characterised by three levels of porosity. The following terms are used in a broad sense in the following: "micropores" refers to intra-aggregate pores in the pellets or powder grains; "macropores" refers to inter-aggregate pores in the pellets or powder grains; "inter-pellet pores" refers to the large pores between pellets and powder grains.

Table 4. Properties of the three pellet-powder mixtures.

Mixture	**70/30**	**70/15**	**70/0**
ρ_d: Mg/m^3	1.50	1.275	1.05
ϕ_{p0}: dimensionless	0.553	0.553	0.553
ϕ_{g0}: dimensionless	0.236	0.118	0

2.3. Imbibition column

The imbibition column was a square cuboid, two faces of which were made of glass. Its inner height was 120 mm (~17.1 times the initial pellet diameter) and its inner width was 60 mm (~8.6 times the initial pellet diameter). The glass faces were made of tempered glass of thickness 9 mm. Their deformation during the test was expected to be negligible such that the imbibition column remained at constant volume.

Four pressure sensors (BER-A-5MP15S from Kyowa, rated capacity of 5 MPa, and accuracy - related to nonlinearity and hysteresis - of 4% of rated output) were used. Three were located on one side at different elevations (20 mm; 60 mm; 100 mm) to measure lateral pressure, one was located at the top face of the column to measure axial pressure. The diameter of all the pressure sensors was 30 mm. The ratio of sensor diameter to pellet diameter was thus ~4.3. The expected coefficient of variation (standard

deviation / mean value) of the measured pressure for this ratio is ~0.1-0.2 (Darde et al., 2021). Four relative humidity sensors (HIH-4000 Series from Honeyweli) were used. Three were located at the same heights as pressure sensors, but on the opposite side, one was located on the top face next to the axial pressure sensor. The accuracy of the relative humidity sensor was +/- 3.5% of the measured value, corresponding to less than 5 MPa of suction for 100% RH at 20°C. Room temperature was controlled and kept constant (20°C ± 1°C).

Porous stones were placed at the top and bottom of the column. A camera was used to take pictures at different moments of all three samples. A sketch of the column is presented in Figure 2.

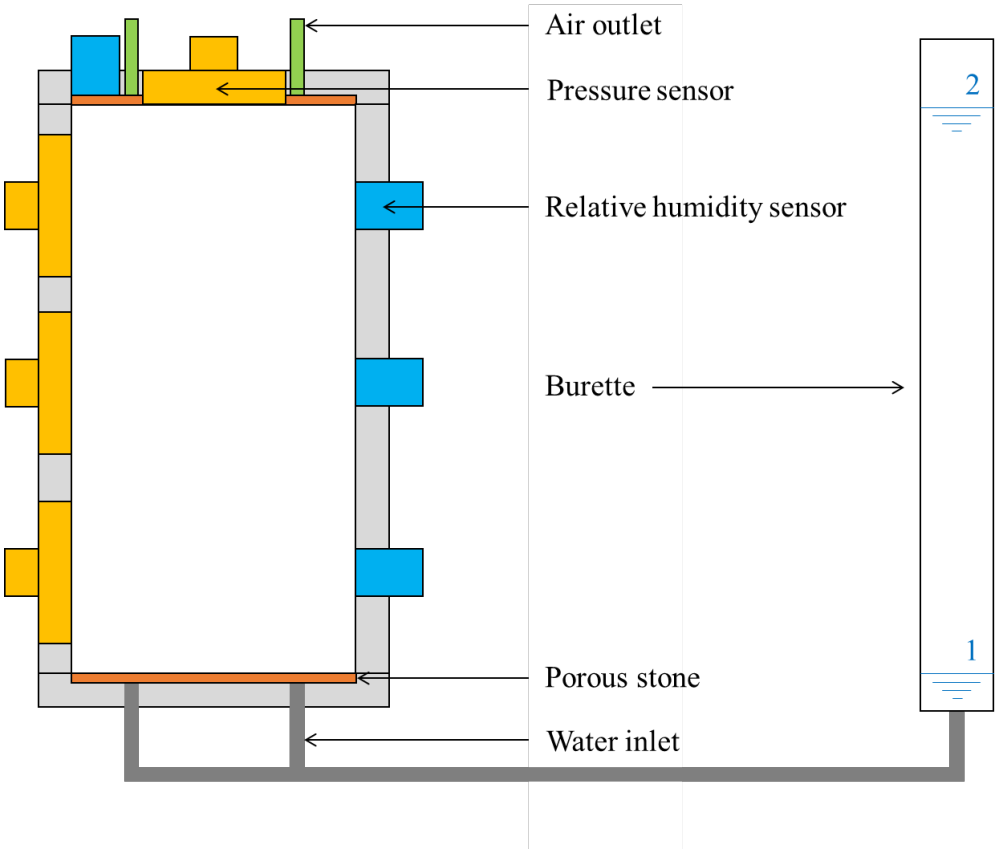

Figure 2. Sketch of the imbibition column, with the water levels associated to each phase of the experiment.

2.4. Sample preparation

During the preparation of the sample, the column was rotated so that a side glass face became the bottom face. The mixtures were then prepared by pouring one layer of pellets, then adding powder in the inter-pellet voids, in a quantity corresponding to the target proportion. This step was repeated to fill the column with the mixture. This procedure was chosen to obtain an initial state as ideally mixed as possible (Molinero-Guerra et al., 2017). Filter papers were used to prevent the occlusion of the porous stones by the powder grains.

Once the column was filled with the mixture, the second glass face was then installed to close the column. During this step, no pressure was applied on the mixture.

The column was finally carefully rotated back to limit powder trickling in the inter-pellet voids. Three experiments are reported in the present work. The three columns were placed side by side to allow pictures of all cells to be taken simultaneously by the camera (Figure 3).

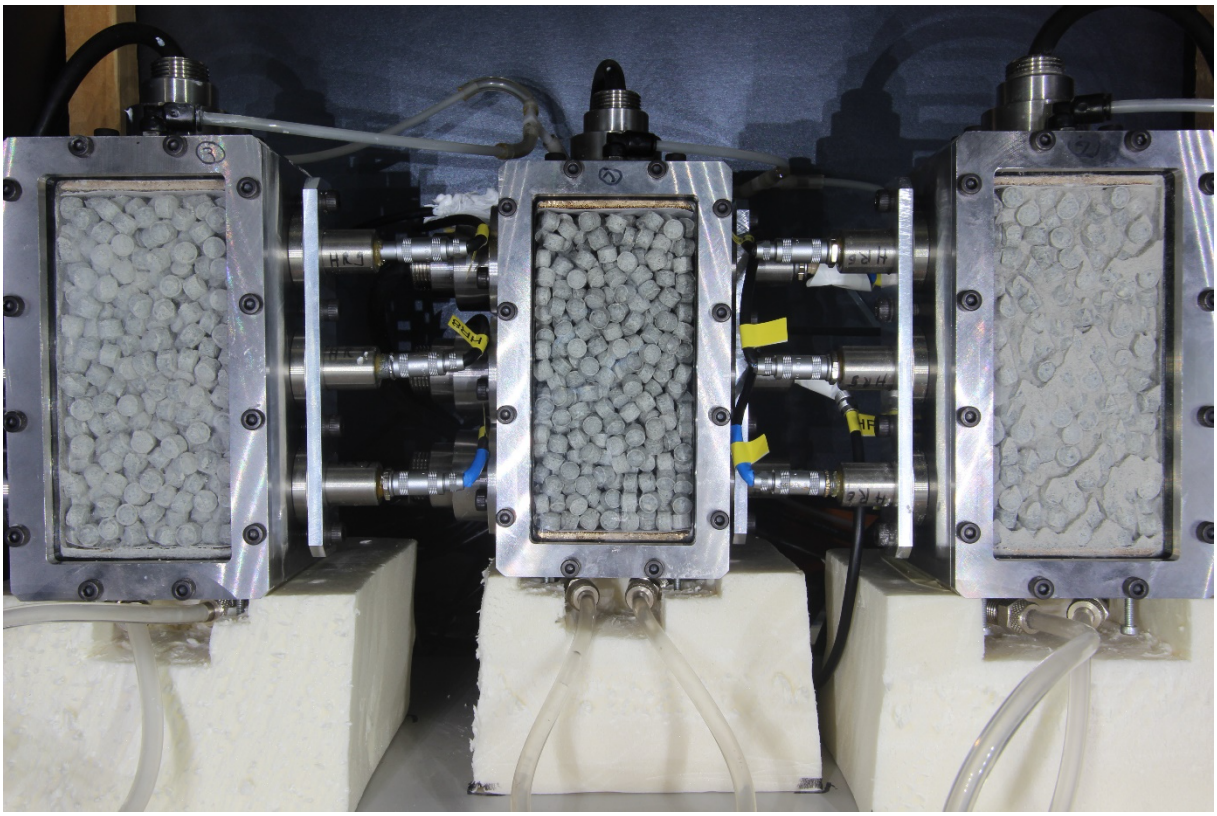

Figure 3. Pellet-powder mixtures in the column following the preparation of the samples. From left to right: 70/15 mixture, 70/0 mixture, 70/30 mixture.

2.5. Imbibition process

The mixture hydration was performed by imbibition of synthetic water from the bottom of the cell. The synthetic water was a solution with the same chemical composition as the pore water of the Callovo-Oxfordian claystone from the underground research laboratory of Andra in Bure, France. The receipt of the water used in experiments is given in Table 5.

Table 5. Receipt of the water used in imbibition experiments.

Salt	Concentration
NaCl	1.95 g/l
$NaHCO_3$	0.130 g/l
KCl	0.035 g/l
$CaSO_4$, $2H_2O$	0.630 g/l
$CaCl_2$, $2H_2O$	0.080 g/l
$MgSO_4$, $7H_2O$	1.020 g/l
Na_2SO_4	0.700 g/l

In the French concept of radioactive waste disposal, the host rock is a claystone, the permeability of which is expected to be below 10^{-17} m² (de la Vaissière et al., 2015). Under repository conditions,

bentonite-based sealing materials are hydrated by the pore water of the host rock. Considering the low permeability of the host rock, hydration is expected to be a slow process.

In this study, imbibition was performed to reproduce the hydration process under repository conditions more realistically: because of the presence of large inter-pellet voids, even a small hydraulic gradient would induce significant water flow rate (Hoffmann et al., 2007) and early loss of the granular structure as a consequence (because of pellet swelling). The volume of incorporated water was measured using a burette.

Imbibition was started when the sensors measured a constant value of relative humidity during several days after the sample preparation, indicating that pellets and powder were at hydraulic equilibrium at the beginning of imbibition. For the first five days of the test, the water level in the burette was maintained at the same level as the bottom porous disk (water level "1" in Figure 2). This allowed the pellets and powder grains in contact with the bottom porous stone to form a thin layer without large inter-pellet voids. Afterwards, the water level was set to the height of the cell (water level "2" in Figure 2). The water head, 120 mm (≈ 1.2 kPa), was small so that the thin homogeneous layer obtained during the first days prevented quick liquid water flow through inter-pellet voids.

The burette was regularly filled with synthetic water during the duration of the test. A small quantity of oil was poured at the top of the water column to prevent evaporation of the water in the burette. Silicone gel was added, between the glass faces and the metal cell, following the cell closure to prevent any leakage during imbibition.

2.6. Measurements of water content and suction

After the end of imbibition tests, suction and water content were measured at different elevations in the samples. Suction was measured using a WP4 dew point potentiameter (Decagon). Water content was measured by oven-drying at 105°C for 24 h. In the following, the term water content is used for the gravimetric water content in the sample.

3. Experimental results

This section presents the results obtained after 640 days of imbibition for the 70/0 and 70/15 mixtures. Because of an experimental issue, the 70/30 test was stopped and dismantled after 235 days, thus results for only 235 days are presented for this mixture. "Final values" reported in the following thus correspond to values measured after 640 days for the 70/0 and 70/15 samples and 235 days for the 70/30 sample.

3.1. Imbibed volume of water

The volume of imbibed water as a function of elapsed time is presented in Figure 4a for the three mixtures, along with horizontal lines corresponding to the estimated total void volume in the samples (including pellet porosity + powder grain porosity + inter-pellet porosity). These values, summarised in Table 6, were estimated from data shown in Table 3 and Table 4. Figure 4b presents the evolution of the water volumetric flow rate during the three tests. It can be observed that the water uptake as well as the water uptake rate were very close between the three tests, despite notable differences in total dry density.

Table 6. Information regarding estimated void volumes in the three tested mixtures.

Mixture	70/30	70/15	70/0
Total porosity: dimensionless	0.458	0.534	0.621
Total void volume: $\times 10^{-4}$ m^3	1.98	2.33	2.68
Saturated water content: dimensionless	0.31	0.42	0.59

The evolution of the imbibed water volume in the three cells followed close trends. The water flow rate monotonically decreased during imbibition. The water flow rate in the experiments can be related to the logarithm of elapsed time with a linear function. This function is the same for the three mixtures. In the 70/15 experiment, progressive clogging of the inlet tube by rust from a screw located at the bottom

of the sample induced a decrease in the water flow (between 350 – 500 days). After changing the tube, the water flow increased again to values comparable to the global trend.

After ~600 days of imbibition, the estimated volume of voids in the sample was reached in samples 70/0 and 70/15. Water intake continued to increase, while the water flow rate continued to decrease.

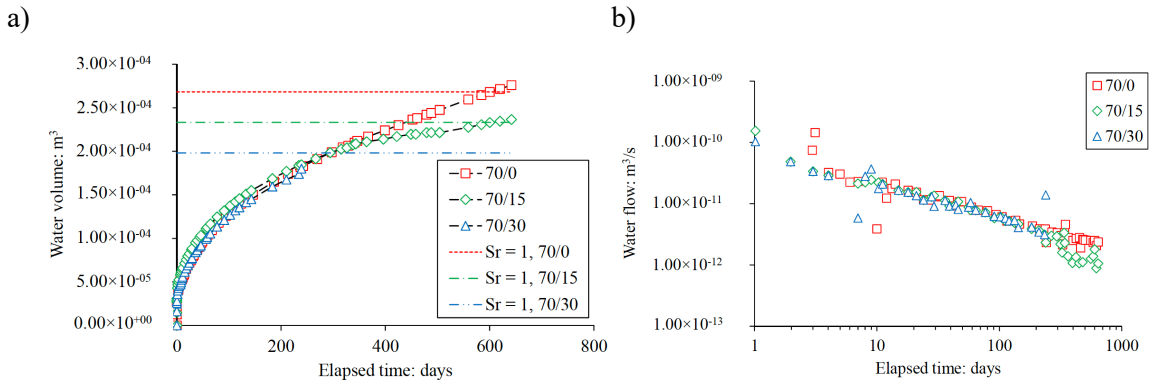

Figure 4. Evolution of a) imbibed water volume and b) water flow rate as functions of elapsed time for the three imbibition tests. Horizontal lines in a) correspond to the estimated total void volume in each sample (Table 6).

3.2. Evolution of the relative humidity

In all three samples, the relative humidity monotonically increased with time during the first 200 days (Figures 5 & 6). The increase in relative humidity at each value of z was slower for samples with higher powder content.

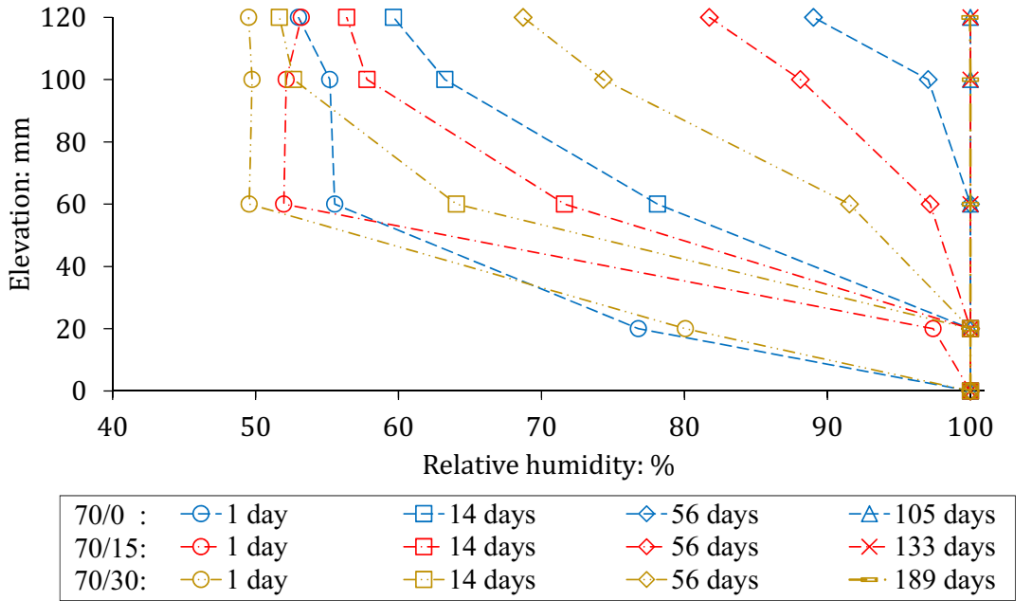

Figure 5. Profiles of relative humidity in the three samples at different times.

The time required for all sensors to obtain a relative humidity of 100% was 105 days for the 70/0 sample, 133 days for the 70/15 sample, and 189 days for the 70/30 sample. Afterwards, the measured relative humidity remained 100% for all the sensors (Figure 6). In addition, the initial suction of the mixtures can be estimated from the measurement of relative humidity. For instant, initial relative humidity was equal to 52-54%, 51-53% and 50% for the samples 70/0, 70/15, and 70/30, respectively. Note that the initial suction of the powder (180 MPa) was higher than that of pellet (89 MPa). Higher powder content should induce thus higher suction (or lower relative humidity) of the mixture.

195

a)

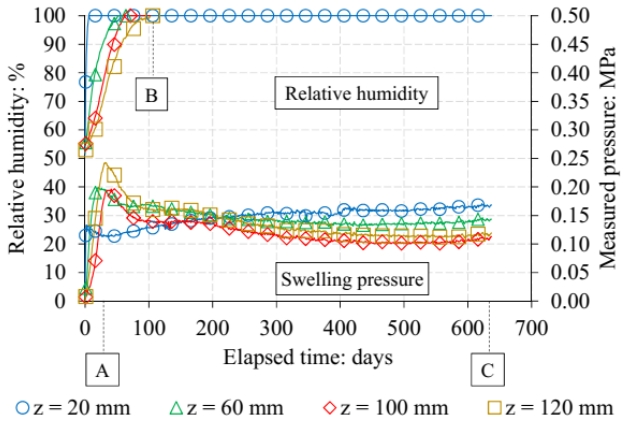
Relative humidity: %
Measured pressure: MPa
Relative humidity
Swelling pressure
Elapsed time: days
A
B
C
z = 20 mm
z = 60 mm
z = 100 mm
z = 120 mm

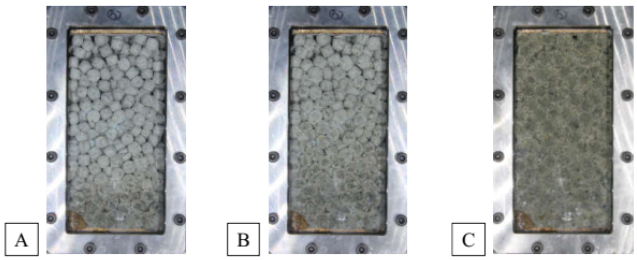
A
B
C

b)

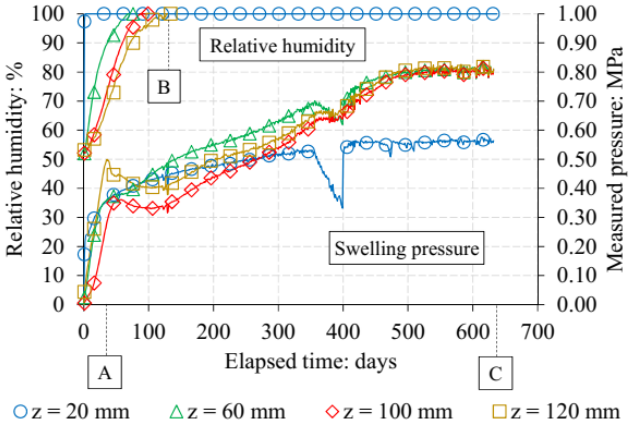
Relative humidity: %
Measured pressure: MPa
Relative humidity
Swelling pressure
Elapsed time: days
A
B
C
z = 20 mm
z = 60 mm
z = 100 mm
z = 120 mm

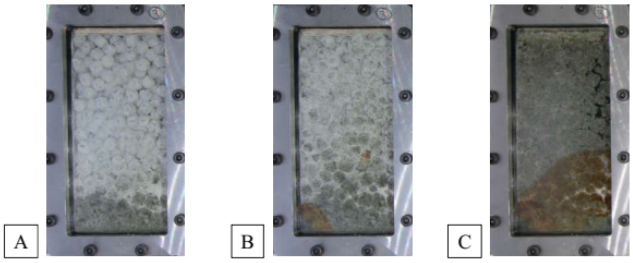
A
B
C

c)

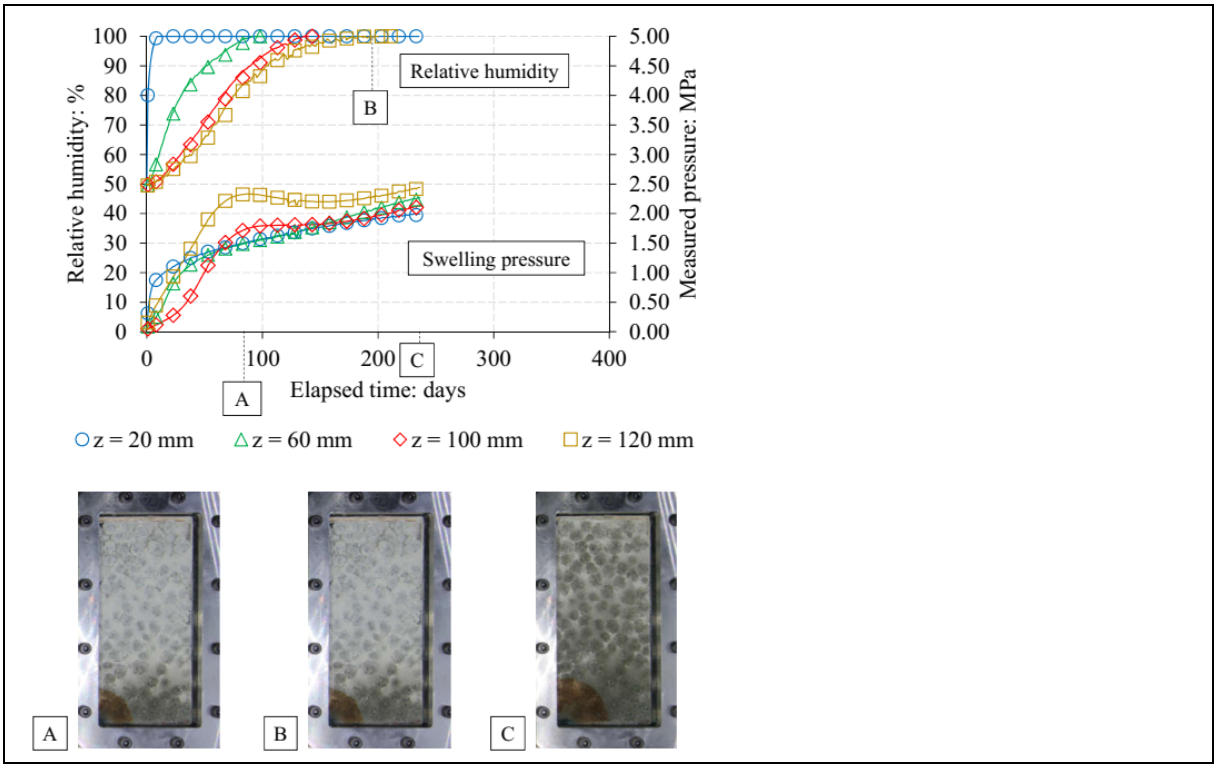

Figure 6. Evolution of the measured pressure, relative humidity, and pictures of the materials at various elapsed times: a) 70/0; b) 70/15; c) 70/30.

3.3. Evolution of the measured pressure

In the 70/0 sample (Figure 6a), lateral pressure increased first close to the water inlet (sensor $z = 20$ mm), at the bottom of the sample. A peak was reached after few days. Afterward, the pressure decreased, stabilised and started to increase from ~50 days. At higher elevations, the measured pressure evolved differently. Axial and lateral pressures increased to higher values and reached sharper peak. Following the peaks, these pressures decreased progressively and slow increase in pressure was observed only from ~500 days.

In the 70/15 sample (Figure 6b), pressures at $z = 20$ mm and $z = 40$ mm increased continuously from the beginning. At higher elevations, the trend was close to that observed in the 70/0 sample, but the increase in the measured pressure following the peak was more significant and occurred earlier (from ~100 days). A transient decrease of pressure was observed before ~400 days by all sensors. This decrease corresponded to a progressive clogging of the water inlet tube identified in the analysis of water intake (Figure 4). After changing the tube, the measured pressures increased again at all elevations.

In the 70/30 sample (Figure 6c), the evolution of pressure close to the water inlet followed a trend comparable to the 70/15 sample. However, at higher elevations, the evolution of the measured pressures was different. Increase of measured pressures was slower and peaks were not as sharp. As in other tests, the highest value of peak pressure was obtained at the top of the sample.

In all samples, the measured pressure continued to increase after relative humidity at all elevations had reached 100% (Figure 6)

3.4. Evolution of the texture of the mixtures

Pictures of the samples, taken during hydration (Figure 6), allowed the evolution of the material textures to be observed and analysed. Three pictures are shown corresponding to the moments when the peak axial pressure was measured at the top of the samples (A), when 100% RH was measured by all sensors (B), and at the end of the test before dismantling (C).

When the peaks of axial pressure were measured at the top of samples 70/0 and 70/15 (moment A in Figure 6a,b), both characterised by sharp decrease of axial pressure (compared to that of sample 70/30),

inter-pellet voids were still clearly observable. The powder grains did not fill all the inter-pellet voids at the top of the 70/15 sample and the top of both 70/0 and 70/15 samples had a clear granular structure. In the 70/30 sample (Figure 6c), inter-pellet voids were completely filled with powder grains when the peak axial pressure was reached. In the three samples, the liquid water front was still at the bottom of the sample. At the bottom of the samples the structure was more homogeneous.

When 100% of relative humidity was reached at all elevations (moment B in Figure 6), large inter-pellet voids were still present at the top of the 70/0 sample (Figure 6a). Conversely, volume of inter-pellet voids decreased because of pellet swelling and a significant part of the inter-pellet voids was filled with powder in the 70/15 sample (Figure 6b). It corresponded to the moment when measured pressures increased again in the 70/15 sample, while they continued to decrease but with a much smaller rate in the 70/0 sample. The texture of the 70/30 material had not significantly evolved when 100% of relative humidity was measured. In all three samples, the liquid water front was still at a low elevation at this moment.

At the end of the test (moment C in Figure 6), the closure of inter-pellet voids was nearly total in the 70/0 sample and total in the other tests. In all samples, the material had lost the initial granular structure but was not completely homogeneous. Besides, some dry pores could be identified in the 70/0 sample, demonstrating that full saturation was not reached.

A dark area spreading from the bottom of the 70/15 sample can be observed on the picture. This was due to rust coming from a screw located at the bottom of the cell, as already mentioned.

3.5. Sample dismantling

At the end of the test, the cells were opened by removing the glass side facing the camera. Following the opening, a utility knife was used to split samples into small portions, in order to measure suction and water content profiles.

The water content profiles of the three samples are presented in Figure 7, along with values of estimated saturated water content as given in Table 6. Saturated water content was estimated with a water density ρ_w = 1.0 Mg/m^3 and a constant value of the mixture dry density. In the three samples, the water content following dismantling was higher at lower elevation.

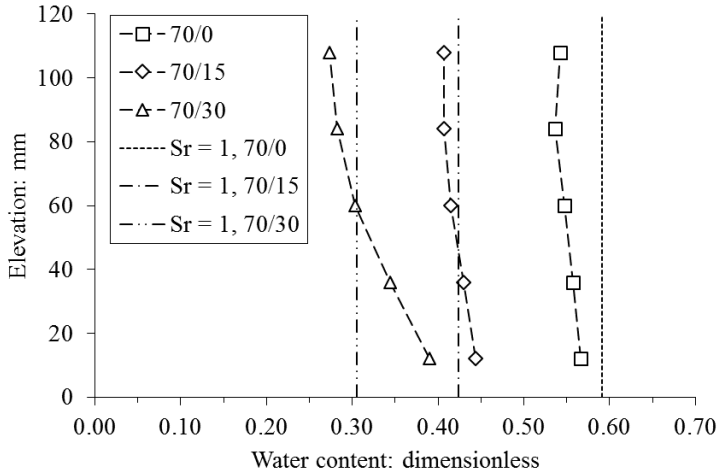

Figure 7. Water content profiles of the three samples following dismantling. "Sr = 1" lines correspond to the estimated water content in fully-saturated state for constant dry density and water density of 1.0 Mg/m^3.

Values of suction (measured by WP4) and water content (determined by oven-drying) were obtained at $z \approx$ 95-120 mm for the 70/0 and 70/15 samples, and $z \approx$ 0-25 mm ; 25-50 mm ; 50-70 mm ; 70-95 mm ; 95-120 mm for the 70/30 sample. The results of water content-suction relationship for the three samples are presented in Figure 8, along with results obtained for a free swelling MX80 7 mm pellet,

identical to those used in the present study (Darde et al., 2018). All the experimental data seem show a unique relationship which could be attributed to the water retention curve of the material.

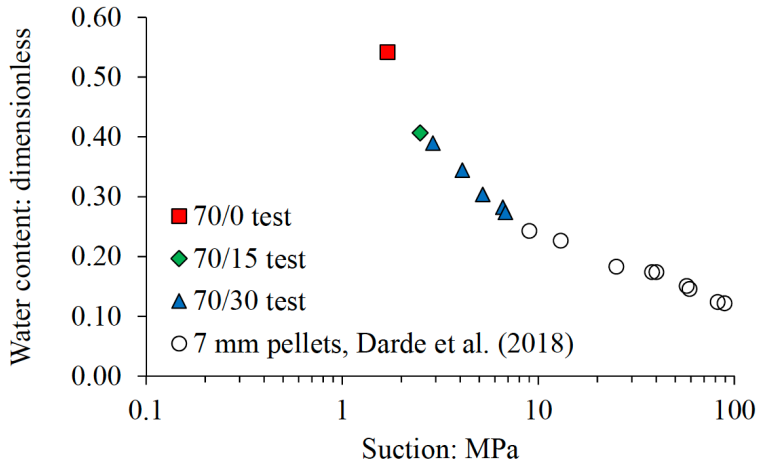

Figure 8. Water content – suction relationship obtained by measures performed on the three samples and a single pellet under free swelling conditions.

4. Discussion

4.1. Choice of experimental apparatus

In this study, imbibition columns were square cuboids with two glass faces. This allowed for the direct observation of the material using a camera. From the existing studies, cylindrical cells have been generally used (e.g. Imbert and Villar, 2006). The cylindrical shape reduces the local deformation; however, it prevents the direct observation of the material. The square cells could induce more deformation of the material in the centre compared to that at the angles. In the present work, pictures taken by the camera did not show significant difference on the behaviour of the material at the angles compared to the other parts.

The use of a second glass face should have allowed the observation of both sides of the cell. Because of space constraint in the laboratory, it was not possible to have cameras on both sides of the cells. Observation of the material evolution on both sides remains an interesting perspective for future experiments.

4.2. Non-measurement of dry density

The profiles of dry density were not determined following dismantling in the present work. The authors considered that experimental constraints (such as the necessity to test a part of sample large enough to contain pellets and powder, the unavoidable small but still non-negligible deformation during sampling, the time required for the measurement, etc.) could affect the relevance of this measurement.

4.3. Slow hydration method

Because of the large inter-pellets pores in the initial state, the permeability of pellet mixtures in the initial state should be high (Hoffmann et al., 2007). Thus, upon fast liquid flooding, water would flow in the large pores, as discussed by Molinero Guerra et al. (2018a), resulting in early loss of granular structure and homogenisation of the mixture. In the present study, it was found that upon slow hydration, the materials could be inhomogeneous even at a relative humidity of 100%. In pellet mixtures, contact interactions between pellets have an influence on the evolution of swelling pressure (Hoffmann et al., 2007; Alonso et al., 2010; Darde et al., 2020b).

4.4. Homogenisation of the mixture upon hydration

The homogenisation of pellet-based bentonite materials reaching fully-saturated state was observed by various authors (Imbert and Villar, 2006; Hoffmann et al., 2007; Molinero Guerra et al., 2018a; Bernachy-Barbe et al., 2020; Darde et al., 2020a). In the present work, taking pictures allowed to follow the progressive loss of the initial granular structure. Under constant-volume conditions, the swelling of the pellet-powder mixture as a whole was prevented. Powder grains thus swelled in inter-pellet voids, the volume of which progressively decreased also as a consequence of pellet swelling, leading to the loss of granular structure. As dismantling was performed before full saturation, the texture did not reach the same degree of homogenisation as in the previously mentioned studies. However, pictures showed that pellets and powder were no longer distinct from each other at the end of the tests.

Dismantling allowed to determine profiles of water content for the three mixtures (Figure 7). In all three mixtures, the water content was higher at a lower elevation. Even if full saturation was not reached, it is worth noting that for the 70/30 sample, the final water content at $z < 60$ mm was higher than the value estimated for the saturated state corresponding to the initial average void ratio. Upon hydration, the bentonite swelled close to the water inlet. Consequently, the void volume following saturation was higher in the zone close to the water inlet. This local swelling close to water inlet could compact the part of the sample further from the water inlet. Thus, even if the texture of the material is expected to reach a full homogenisation at full saturation, inhomogeneous profiles of water content and densities are to be expected in pellet-based bentonite materials as in other bentonite materials.

Axial and lateral pressures were not similar in the samples at the end of the tests. Even if further evolution was still expected because the samples were not fully-saturated, disparity of the measured pressure has been observed in the literature (Molinero Guerra et al., 2018b; Dueck et al., 2019; Bernachy-Barbe et al., 2020; Bernachy-Barbe, 2021). Swelling pressure was affected by the initial heterogeneities of density of the sample (Molinero Guerra et al., 2020), as well as by the non-homogeneous hydration as previously discussed. In addition, friction between bentonite and the cell walls may contribute to the difference between axial and lateral pressures (Bernachy-Barbe, 2021). Such heterogeneities of measured pressure were also obtained in experiments performed on compacted bentonite block (Saba et al., 2014).

4.5. Influence of the granular structure

The use of cells with glass sides allows to observe the progressive evolution of the material structure from the initial state. It provides a complementary "qualitative" information to sensor "quantitative" measurements like values of measured pressure and relative humidity, which brings insight into the mechanical behaviour of pellet-based bentonite materials under repository conditions.

Pictures taken by the camera (Figure 6) showed that the peak axial pressure measured at the top of the sample for 70/0 and 70/15 was reached when the material structure was characterised by large inter-pellet pores. Conversely, the inter-pellet pores in the 70/30 sample at peak axial pressure measured at the top of the sample were completely filled with powder. Besides, after 133 days for the 70/15 sample and 189 days for the 70/30 sample, when measured axial and lateral pressures were increasing following the peak in both samples, inter-pellet pores were filled with powder.

Figure 9 presents the peak pressures measured during hydration in all samples as functions of suction, converted from relative humidity measured at the same height using the Kelvin law. Two distinct trends can be observed: high pressure peaks were obtained in the 70/30 sample; and low swelling pressure peaks were obtained in the 70/0 and 70/15 samples. Along with experimental results, the mean stress corresponding to pellet failure in a pellet assembly without powder, determined by Darde et al. (2021), was plotted in a dashed line. The low swelling pressure peaks, obtained in samples with an observable granular structure (which were considered in the numerical simulation performed by Darde et al. 2021 using DEM), were close to this line. That confirmed the dominant role of granular structure on swelling pressure for these samples. Note that the variability of the measurement of suction was expected to be lower than 5 MPa, such that these trends are not considered affected by sensor accuracy. In addition, the diameter of the pressure sensors was taken four times as large as the pellet so that measured pressures are considered accurate.

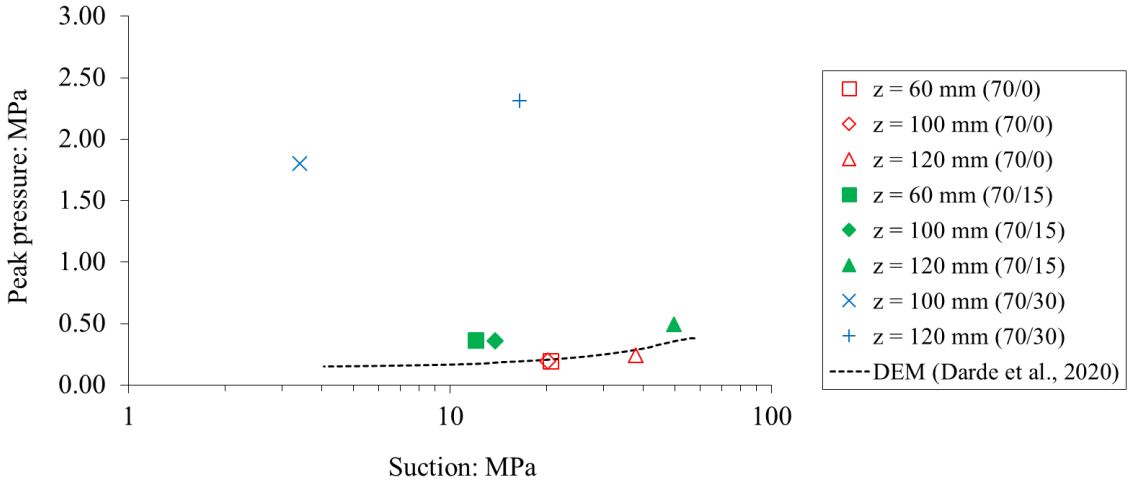

Figure 9. Peak pressure measured in the three samples plotted as a function of suction, determined from relative humidity measurement and the Kelvin law. The dashed line is the mean stress corresponding to pellet strength in a pellet assembly as determined by Darde et al. (2021) using Discrete Element Method.

Measurement of a peak of pressure was described in other studies about hydration of bentonite-based materials under constant volume conditions. In clayey materials compacted on the dry side of optimum compaction (i.e. water content smaller than optimum water content), clay particles (basically stacks of lamellae) form aggregates, resulting in a well-documented double structure (Pusch, 1982; Delage et al., 1996; Lloret et al., 2003; Cuisinier and Laloui, 2004; Romero and Simms, 2008). Bentonite hydration results from the progressive adsorption of water molecules around the cations in the interlayer (Norrish, 1954; Sposito and Prost, 1982; Torikai et al., 1996; Saiyouri et al., 2004; Jacinto et al., 2012), inducing clay particles swelling and decrease of aggregate stability. At high water contents, the aggregate structure is no longer stable, collapses, and macropores are filled with exfoliated clay lamellae (Keller et al., 2015; Massat et al., 2016). The hydration mechanism then becomes related to the development of diffuse double layers (Saiyouri et al., 2000; Delage et al., 2006).

Under constant-volume conditions, these mechanisms can result in the development of a peak swelling pressure related to the collapse of the aggregated structure, followed by another increase to a final value (Lloret et al., 2003). As reported by Lloret et al., (2003), the decrease of swelling pressure resulting from this phenomenon was observed if the level of stress was sufficiently high, and thus may not be observed in low dry density samples. Peaks of pressure were also measured in pellet-based bentonite materials as discussed by others studies (Imbert and Villar, 2006; Alonso et al., 2011; Molinera Guerra et al., 2018b; Benarchy-Barbe et al., 2020).

Because of the initial granular structure, the evolution of the measured pressure of pellet materials can be different from that of compacted blocks. Before losing the initial granular structure upon hydration, the macroscopic pressure developed in a pellet assembly results from an increase of number of contacts between grains and the pressure sensor and the magnitude of force at these contacts. If contact forces reach pellet strength, they remain constant (perfect plasticity behaviour), while the pellet stiffness continues to decrease upon hydration, inducing swelling pressure decrease (Darde et al., 2021). Results of the present study suggest that, in mixtures of pellet and powder, the cause of the transient decrease of swelling pressure depends on the powder content.

In low powder content mixtures, the powder does not completely fill the inter-pellet pores. Its initial contribution to the mechanical behaviour is negligible (Darde et al., 2020a). Pressure development is related to the increase in contact forces between pellets, and a peak of pressure occurs if contact forces reach the pellet strength. Following the peak, pellets and powder continue to swell. The contribution of powder progressively becomes significant and overcomes that of contact forces between pellets. The material behaviour is then comparable to that of a continuous material. Results obtained for the 70/15 sample can be explained by this interpretation (Figure 9).

In high powder content mixtures, the powder fills the inter-pellet pores. Its contribution to the mechanical behaviour of the mixture cannot be neglected. Swelling pressure is not directly related to contact forces between pellets. The pellet assembly does not control the mechanical behaviour. Peak pressure is thus interpreted as the collapse of the aggregate structure, as continuous bentonite materials. Results obtained for the 70/30 sample can be explained by this interpretation. Besides, Imbert and Villar (2006) concluded that a mixture of pellets and powder in 50/50 proportions did not behave differently than continuous bentonite materials of same dry density.

4.6. Water migration process

The saturated permeability in compacted bentonite was shown to be related to its dry density (Karnland et al., 2006; Lloret and Villar, 2007). It suggests that under fully-saturated conditions, water flows through the macropores of the bentonite. In the present study, three different mixtures of pellets and powder were studied. The initial dry densities of these mixtures were 1.05 Mg/m^3; 1.275 Mg/m^3; and 1.50 Mg/m^3. Under saturated conditions, it was expected that permeability, thus water flow under comparable gradients of water potential, would be significantly higher for lower dry densities.

In Figure 4, for the three samples, the flow rate of water entering the three samples was comparable, regardless of the mixture dry density. Besides, it was observed that the liquid water front was at a low elevation when all sensors measured a relative humidity of 100%. Air-filled inter-pellet pores could be observed in pictures taken by the camera. These observations suggest that the dominant water migration mechanism under unsaturated conditions was not liquid flow in the macropores (inter-aggregate pores in the pellets or powder grains). Two other mechanisms can be proposed to explain the saturation of the material. The first mechanism is liquid water flow through the micropores (intra-aggregate pores in the pellets or powder grains). The second mechanism is vapour water flow in the macropores and inter-pellet pores. The flow rate of water entering the sample was thus controlled by: (*i*) liquid flux in the micropores, affected by strong solid-water interactions (Komine, 2008); (*ii*) the rate at which the liquid water undergoes phase change to vapour at the interface between the saturated and unsaturated zones (Lozano et al., 2008; Ouedraogo et al., 2013). Both phenomena can be considered independent of dry density.

Comparison of Figure 4 and Figure 6 **Error! Reference source not found.** provides interesting additional information about the hydration of the mixtures. The volume of water imbibed by the samples continued to increase in all samples after all sensors measured a 100% relative humidity in the inter-pellet pores. Thus, the bentonite continued to take up water. It confirms that diffusive migration of water vapour was faster in the large inter-pellet space than in the micropores of the pellet. Kröhn (2005) also proposed vapour migration as the main saturation mechanism in compacted bentonites. Besides, it means that pellets and inter-pellet pores were not at hydraulic equilibrium during saturation. The increase in measured pressure following the measurement of 100% relative humidity was also consistent with this suggestion. On another note, even if the material was not saturated when dismantled, the imbibed volume of water was higher than the estimated volume of voids (Figure 4). Similar results have been already observed by Wang et al. (2013). A possible interpretation is the increase of density of the water adsorbed on the surface of clay lamellae, as already suggested in the literature (Lloret and Villar, 2007; Jacinto et al., 2012; Molinero Guerra et al., 2018b). Another possible explanation would be a leak in the system, despite the care taken to avoid leakage, or the volume of water required to fill the ducts and porous plate at the bottom of the column was underestimated.

The size of powder grains was smaller than that of pellets. Consequently, a decrease in the relative humidity of the surrounding air (pore between grains or pellets) would induce a faster decrease of relative humidity in the whole powder grain than in the whole pellet. In Figure 6, progress of vapour diffusing in the pore air is shown to be slower in mixtures with higher powder content. It suggests that hydration of powder grains occurred simultaneously with vapour migration in the inter-pellet pores. This hydration consumed water, and thus slowed down the apparent rate of vapor diffusion throughout mixtures containing powder. It is consistent with the profiles of water content following dismantling (Figure 7): the differences of water contents measured at low and high elevations were less significant

in the mixture with no powder, where vapour could diffuse in the large inter-pellet pores with no powder. The delay of hydration and hydraulic disequilibrium between micropores and inter-pellet pores is thus considered to be mostly related to pellets.

Figure 10 presents a summary of the interpretations of experimental results regarding the water migration in the samples during the saturation.

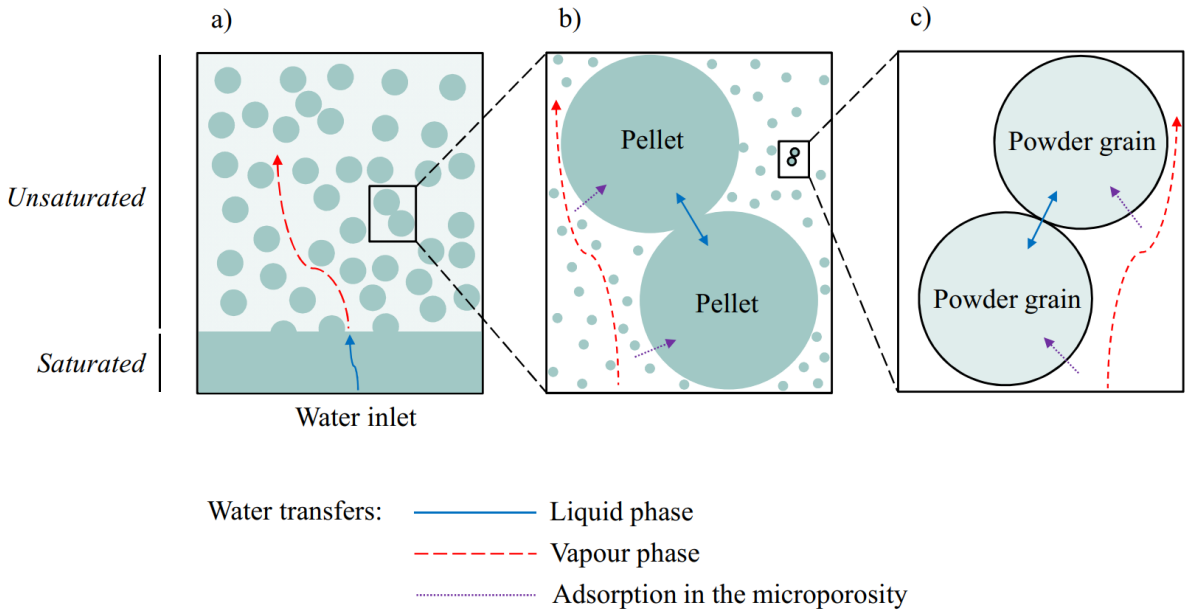

Figure 10. Interpretation of the water migration mechanisms in the samples: a) at the imbibition cell scale; b) at the pellet scale; c) at the powder grain scale.

The present discussion suggests that, despite the very high initial permeability of the material, water flow in liquid phase through inter-pellet space is very unlikely before full saturation of the buffer under repository conditions, in concepts with a low permeability host rock such as claystone.

5. Conclusion

The present study investigated the hydromechanical behaviour of pellet-powder mixtures through imbibition experiments in the laboratory. A hydration column was specially designed, with glass sides, allowing pictures of the sample to be taken during hydration, along with measurements of relative humidity and swelling pressure at different elevations. The experiments allowed the transient behaviour of pellet-powder mixtures to be studied under conditions close to repository conditions by avoiding significant liquid water flow rates in the large inter-pellet voids. Swelling pressure was measured by using sensors four times as large as the pellets to decrease the measurement variability. Three mixtures with identical pellet volume fractions (with respect to the total volume) and various powder volume fractions were tested to study the influence of heterogeneities of density in the repository.

In this regard, the present study provides an insight into the behaviour of pellet-powder mixtures under repository conditions, the influence of heterogeneities of density, water migration mechanisms, and progressive homogenisation of the initial structure. The following conclusions can be drawn from the present work:

- (*i*) The average dry density of the material did not influence the water flow entering the samples under unsaturated conditions;

- (*ii*) The evolution of pressure, including the occurrence of a peak, was consistent with an increase in contact number between pellets (and the forces at these contacts) for samples with low powder content;
- (*iii*) The material progressively lost the initial granular structure during hydration;
- (*iv*) Pellets and inter-pellet pores were not at hydraulic equilibrium during imbibition;
- (*v*) Vapour migration was expected to be the dominant mechanism of saturation of the pellet-powder mixtures investigated in this study.

In depth analysis of the homogenisation process in pellet mixtures based on the pictures, and relevant comparison of the swelling pressure development in bentonite pellet mixtures and compacted blocks of same dry density thanks to the large pressure sensors are two interesting perspectives of the present work.

Declaration of competing interests

The authors declare that they have no known competing financial interests or personal relationships that could have appeared to influence the work reported in this paper.

List of references

Alonso, E.E., Hoffmann, C., Romero, E., 2010. Pellet mixtures in isolation barriers. J. Rock Mech. Geotech. Eng. 2, 12–31. https://doi.org/10.3724/SP.J.1235.2010.00012

Alonso, E.E., Romero, E., Hoffmann, C., 2011. Hydromechanical behaviour of compacted granular expansive mixtures: experimental and constitutive study. Géotechnique 61, 329–344. https://doi.org/10.1680/geot.2011.61.4.329

Andra, 2005. Dossier 2005 Argile, Synthesis. Evaluation of the feasibility of a geological repository in an argillaceous formation. Meuse/Haute-Marne site. 238 pages.

Bernachy-Barbe, F., Conil, N., Guillot, W., Talandier, J., 2020. Observed heterogeneities after hydration of MX-80 bentonite under pellet/powder form. Appl. Clay Sci. 189, 105542. https://doi.org/10.1016/j.clay.2020.105542

Bernachy-Barbe, F., 2021. Homogenization of bentonite upon saturation: Density and pressure fields. Applied Clay Science, 209, 106122.

Bosgiraud, J.M., Foin, R., 2016. DOPAS WP3 Deliverable D3.7. Test report on FSS metric clayish material emplacement tests with clayish material definition and laboratory work on its performance. 35 pages.

Cuisinier, O., Laloui, L., 2004. Fabric evolution during hydromechanical loading of a compacted silt. Int. J. Numer. Anal. Methods Geomech. 28, 483–499. https://doi.org/10.1002/nag.348

Darde, B., Tang, A.M., Pereira, J.-M., Roux, J.-N., Dangla, P., Talandier, J., Vu, M.N., 2018. Hydro-mechanical behaviour of high-density bentonite pellet on partial hydration. Géotechnique Lett. 8, 330–335. https://doi.org/10.1680/jgele.18.00114

Darde, B., Dangla, P., Roux, J., Pereira, J., Talandier, J., Vu, M.N., Tang, A.M., 2020a. Modelling the behaviour of bentonite pellet-powder mixtures upon hydration from dry granular state to saturated homogeneous state. Eng. Geol. 278, 105847. https://doi.org/10.1016/j.enggeo.2020.105847

Darde, B., Tang, A.M., Roux, J.-N., Dangla, P., Pereira, J.-M., Talandier, J., Vu, M.N., 2020b. Effects of the initial granular structure of clay sealing materials on their swelling properties: experiments and DEM simulations. Eur. Phys. J. Nucl. Sci. Technol. 6, 1. https://doi.org/10.1051/epjn/2019059

Darde, B., Roux, J.-N., Pereira, J.-M., Dangla, P., Talandier, J., Vu, M.N., Tang, A.M., 2021. Investigating the hydromechanical behaviour of bentonite pellets by swelling pressure tests and discrete element modelling. Acta Geotechnica, 16, 507 - 524. https://doi.org/10.1007/s11440-020-

01040-5

de la Vaissière, R., Armand, G., Talandier, J., 2015. Gas and water flow in an excavation-induced fracture network around an underground drift: A case study for a radioactive waste repository in clay rock. J. Hydrol. 521, 141–156. https://doi.org/10.1016/j.jhydrol.2014.11.067

Delage, P., Audiguier, M., Cui, Y.J., Howat, M.D., 1996. Microstructure of a compacted silt. Can. Geotech. J. 33, 150–158.

Delage, P., Marcial, D., Ruiz, X., Cui, Y.J., 2006. Ageing effects in a compacted bentonite: a microstructure approach. Géotechnique 56, 291–304. https://doi.org/10.1680/geot.2006.56.5.291

Dixon, D., Sanden, T., Jonsson, E., Hansen, J., 2011. Backfilling of deposition tunnels: use of bentonite pellets. SKB P-11-44. 52 pages.

Dueck, A., Börgesson, L., Goudarzi, R., 2019. Bentonite Homogenisation - Laboratory study of homogenisation processes in buffer and backfill materials in repositories. Journal of Earth Sciences and Geotechnical Engineering, 9(3), 165 - 197.

Hoffmann, C., Alonso, E.E., Romero, E., 2007. Hydro-mechanical behaviour of bentonite pellet mixtures. Phys. Chem. Earth 32, 832–849. https://doi.org/10.1016/j.pce.2006.04.037

Imbert, C., Villar, M.V., 2006. Hydro-mechanical response of a bentonite pellets/powder mixture upon infiltration. Appl. Clay Sci. 32, 197–209. https://doi.org/10.1016/j.clay.2006.01.005

Jacinto, A.C., Villar, M. V., Ledesma, A., 2012. Influence of water density on the water-retention curve of expansive clays. Géotechnique 62, 657–667. https://doi.org/10.1680/geot.7.00127

Karnland, O., Olsson, S., Nilsson, U., 2006. Mineralogy and sealing properties of various bentonites and smectite-rich clay materials. SKB Tech. Rep.

Kaufhold, S., Baille, W., Schanz, T., Dohrmann, R., 2015. About differences of swelling pressure - dry density relations of compacted bentonites. Appl. Clay Sci. 107, 52–61. https://doi.org/10.1016/j.clay.2015.02.002

Keller, L.M., Holzer, L., Gasser, P., Erni, R., Rossell, M.D., 2015. Intergranular pore space evolution in MX80 bentonite during a long-term experiment. Appl. Clay Sci. 104, 150–159. https://doi.org/10.1016/j.clay.2014.11.024

Komine, H., 2008. Theoretical equations on hydraulic conductivities of bentonite-based buffer and backfill for underground disposal of radioactive wastes. J. Geotech. Geoenvironmental Eng. 134, 497–508. https://doi.org/10.1061/(ASCE)1090-0241(2008)134:4(497)

Kröhn, K.P., 2005. New evidence for the dominance of vapour diffusion during the re-saturation of compacted bentonite. Eng. Geol. 82, 127–132. https://doi.org/10.1016/j.enggeo.2005.09.015

Lloret, A., Villar, M. V., 2007. Advances on the knowledge of the thermo-hydro-mechanical behaviour of heavily compacted “FEBEX” bentonite. Phys. Chem. Earth 32, 701–715. https://doi.org/10.1016/j.pce.2006.03.002

Lloret, A., Villar, M. V, Sanchez, M., Gens, A., Pintado, X., Alonso, E., 2003. Mechanical behaviour of heavily compacted bentonite under high suction changes. Geotechnique 53, 27–40. https://doi.org/10.1680/geot.53.1.27.37258

Lozano, A., Cherblanc, F., Cousin, B., Benet, J., 2008. Experimental study and modelling of the water phase change kinetics in soils. Eur. J. Soil Sci. 59, 939–949. https://doi.org/10.1111/j.1365-2389.2008.01050.x

Massat, L., Cuisinier, O., Bihannic, I., Claret, F., Pelletier, M., Masrouri, F., Gaboreau, S., 2016. Swelling pressure development and inter-aggregate porosity evolution upon hydration of a compacted swelling clay. Appl. Clay Sci. 124–125, 197–210.

548 https://doi.org/10.1016/j.clay.2016.01.002

549 Molinero Guerra, A., Mokni, N., Delage, P., Cui, Y.J., Tang, A.M., Aimedieu, P., Bernier, F., Bornert,
550 M., 2017. In-depth characterisation of a mixture composed of powder/pellets MX80 bentonite.
551 Appl. Clay Sci. 135, 538–546. https://doi.org/10.1016/j.clay.2016.10.030

552 Molinero Guerra, A., Aimedieu, P., Bornert, M., Cui, Y.J., Tang, A.M., Sun, Z., Mokni, N., Delage, P.,
553 Bernier, F., 2018a. Analysis of the structural changes of a pellet/powder bentonite mixture upon
554 wetting by X-ray computed microtomography. Appl. Clay Sci. 165, 164–169.
555 https://doi.org/10.1016/j.clay.2018.07.043

556 Molinero Guerra, A., Cui, Y.J., Mokni, N., Delage, P., Bornert, M., Aimedieu, P., Tang, A.M., Bernier,
557 F., 2018b. Investigation of the hydro-mechanical behaviour of a pellet/powder MX80 bentonite
558 mixture using an infiltration column. Eng. Geol. 243, 18–25.
559 https://doi.org/10.1016/j.enggeo.2018.06.006

560 Noiret, A., Bethmont, S., Bosgiraud, J., Foin, R., 2016. DOPAS Work Package 4 Deliverable 4.8 FSS
561 Experiment Summary Report.

562 Norrish, K., 1954. The swelling of montmorillonite. Discuss. Faraday Soc. 18, 120–134.
563 https://doi.org/10.1039/DF9541800120

564 Ouedraogo, F., Cherblanc, F., Naon, B., Bénet, J.C., 2013. Water transfer in soil at low water content.
565 Is the local equilibrium assumption still appropriate? J. Hydrol. 492, 117–127.
566 https://doi.org/10.1016/j.jhydrol.2013.04.004

567 Pusch, R., 1982. Mineral-water interactions and their influence on the physical behavior of highly
568 compacted Na bentonite. Can. Geotech. J. 19, 381–387. https://doi.org/10.1139/t82-041

569 Romero, E., Simms, P.H., 2008. Microstructure investigation in unsaturated soils: A review with special
570 attention to contribution of mercury intrusion porosimetry and environmental scanning electron
571 microscopy. Geotech. Geol. Eng. 26, 705–727. https://doi.org/10.1007/978-1-4020-8819-3_8

572 Saba, S., Cui, Y.J., Tang, A.M., Barnichon, J., 2014. Investigation of the swelling behaviour of
573 compacted bentonite-sand mixtures by mock-up tests. Can. Geotech. J. 51, 1399–1412.

574 Saiyouri, N., Hicher, P.Y., Tessier, D., 2000. Microstructural approach and transfer water modelling in
575 highly compacted unsaturated swelling clays. Mech. Cohesive-frictional Mater. 5, 41–60.

576 Saiyouri, N., Tessier, D., Hicher, P.Y., 2004. Experimental study of swelling in unsaturated compacted
577 clays. Clay Miner. 39, 469–479. https://doi.org/10.1180/0009855043940148

578 Sánchez, M., Gens, A., Villar, M.V., Olivella, S., 2016. Fully Coupled Thermo-Hydro-Mechanical
579 Double-Porosity Formulation for Unsaturated Soils. Int. J. Geomech. D4016015.
580 https://doi.org/10.1061/(ASCE)GM.1943-5622.0000728

581 Sellin, P., Westermark, M., Leupin, O., Norris, S., Gens, A., Wieczorek, K., Talandier, J., Swahn, J.,
582 2020. Beacon: bentonite mechanical evolution. EPJ Nuclear Sci. Technol. 6, 23.
583 https://doi.org/10.1051/epjn/2019045

584 Sposito, G., Prost, R., 1982. Structure of Water Adsorbed on Smectites. Chem. Rev. 82, 553–573.
585 https://doi.org/10.1021/cr00052a001

586 Torikai, Y., Sato, S., Ohashi, H., 1996. Thermodynamic Properties of Water in Compacted Sodium
587 Montmorillonite. Nucl. Technol. 115, 73–80.

588 van Geet, M., Volckaert, G., Roels, S., 2005. The use of microfocus X-ray computed tomography in
589 characterising the hydration of a clay pellet/powder mixture. Appl. Clay Sci. 29, 73–87.
590 https://doi.org/10.1016/j.clay.2004.12.007

591 Villar, M.V., Iglesias, R.J., Gutierrez-Alvarez, C., Carbonell, B., 2021. Pellets/block bentonite barriers:

Laboratory study of their evolution upon hydration. Engineering Geology, 292, 106272.

Wang, Q., Tang, A.M., Cui, Y.J., Delage, P., Gatmiri, B., 2012. Experimental study on the swelling behaviour of bentonite/claystone mixture. Eng. Geol. 124, 59–66. https://doi.org/10.1016/j.enggeo.2011.10.003

Wang, Q., Tang, A.M., Cui, Y.J., Barnichon, J.D., Ye, W.M., 2013. A comparative study on the hydro-mechanical behaviour of compacted bentonite/sand plug based on laboratory and field infiltration tests. Engineering Geology, 162, 79 - 87.

List of Figures

List of Tables